

The Phase Structure of the Polyakov–Quark-Meson Model

B.-J. Schaefer,^{1,*} J.M. Pawłowski,^{2,†} and J. Wambach^{3,4,‡}

¹*Institut für Physik, Karl-Franzens-Universität Graz, Universitätsplatz 5, A-8010 Graz, Austria*

²*Institut für Theoretische Physik, Universität Heidelberg,
Philosophenweg 16, D-69120 Heidelberg, Germany*

³*Institut für Kernphysik, TU Darmstadt, Schloßgartenstr. 9, D-64289 Darmstadt, Germany*

⁴*Gesellschaft für Schwerionenforschung mbH, Planckstr. 1, D-64291 Darmstadt, Germany*

The relation between the deconfinement and chiral phase transition is explored in the framework of an Polyakov-loop-extended two-flavor quark-meson (PQM) model. In this model the Polyakov loop dynamics is represented by a background temporal gauge field which also couples to the quarks. As a novelty an explicit quark chemical potential and N_f -dependence in the Polyakov loop potential is proposed by using renormalization group arguments. The behavior of the Polyakov loop as well as the chiral condensate as function of temperature and quark chemical potential is obtained by minimizing the grand canonical thermodynamic potential of the system. The effect of the Polyakov loop dynamics on the chiral phase diagram and on several thermodynamic bulk quantities is presented.

PACS numbers: 12.38.Aw

I. INTRODUCTION

Driven by the heavy-ion programs at GSI, CERN SPS, RHIC and soon the LHC there is strong interest in the properties of strongly interacting matter at extreme temperatures and baryon densities. Ultimately these have to be understood on the basis of Quantum Chromodynamics (QCD), which governs the strong interaction sector of the Standard Model.

QCD at zero temperature and density is well-established by now both numerically and analytically. Besides numerical evaluations on discrete space-time lattices, e.g. [1, 2], functional methods based on the Functional Renormalization Group (FRG), e.g. [3, 4], and Dyson-Schwinger equations (DSE), e.g. [5], have been used to elucidate our understanding of the theory of strong interactions. If applicable, lattice computations give high numerical accuracy with small truncation errors. Functional methods have their advantages if it comes to the deep infrared, the simple explanation of physical mechanisms as well as the inclusion of chiral dynamical quarks. The last years have seen a very fruitful interaction between the different methods leading to a largely quantitative understanding of QCD at vanishing temperature and density even though the full under-

standing of the confinement mechanism and its relation to spontaneous chiral symmetry breaking is not yet settled.

At finite temperature and in particular at finite baryon density or chemical potential μ_B the situation is much less clear. At finite μ_B lattice computations have principal limitations due to the complex action which hampers stringent theoretical evaluations of the QCD phase diagram, in particular the possible critical endpoint of the line of first-order transitions from first principles. Functional methods have been used to obtain results for pure Yang-Mills at finite temperature, as well as the hadronic sector of QCD at finite temperature and density, see e.g. [3, 4]. A full QCD study is hampered by the fact that the gauge sector, i.e. the confinement-deconfinement phase transition in pure Yang-Mills, is not fully resolved yet: the potential for the order parameter, the Polyakov loop, does not lead to a phase transition in perturbative computations, e.g. [6, 7, 8], but recently this gap has been closed within a non-perturbative flow study [9]. Hence, a first principle approach to QCD at finite temperature and density with functional methods is in reach. In our opinion this opens a way to continuing the fruitful interaction between the different methods that has already proven so successful at vanishing temperature.

A first step towards a full QCD study with functional methods is done by studying effective Lagrangian models which are constructed from the non-perturbative Yang-Mills effective potential and effective hadronic models. In recent years a promising realization of this idea has

*Electronic address: bernd-jochen.schaefer@uni-graz.at

†Electronic address: j.pawłowski@thphys.uni-heidelberg.de

‡Electronic address: wambach@physik.tu-darmstadt.de

been put forward, based on lattice results for the thermodynamic potential in pure Yang-Mills (YM) theory and universality arguments [10, 11, 12, 13, 14, 15, 16, 17, 18, 19, 20, 21]. Pure YM theory corresponds to the heavy-quark limit of QCD in which the Polyakov loop expectation value serves as an order parameter for confinement. This approach results in an effective scalar Z_{N_c} -theory whose physical minima are the vacuum expectation values of the Polyakov loop. It has been observed that a thermodynamic potential for the Polyakov loop can be constructed where the parameters are fitted to precise finite-temperature lattice data for the equation of state (EoS) in the heavy-quark limit. This very successful theory simulates the calculated first-order confinement-deconfinement phase transition at finite temperature. For two light flavors, on the other hand, QCD exhibits an (almost) exact chiral symmetry and is believed to be in same universality class as the $O(4)$ model [22]. An effective realization of this symmetry is provided by the Nambu-Jona-Lasinio (NJL) model or, upon bosonization, the quark-meson (QM) model. It is therefore natural to combine both aspects of QCD by coupling light chiral quarks to the Polyakov loop field. This results in the PNJL model [14, 18, 21, 23, 24] or the PQM model, which has the benefit of renormalizability, and a simpler linkage to full QCD, see e.g. [25]. Calculations for the thermodynamic potential and the resulting phase structure will be performed at the mean-field level as was done in similar analyses using the PNJL model. Eventually, however, we plan to include fluctuations using RG-techniques [26].

Even at the mean-field level there remain some open issues. First of all, the Polyakov loop potentials suggested so far, are fixed at vanishing μ_B . In this case, the expectation value Φ of the Polyakov loop operator and that of its adjoint, $\bar{\Phi}$ are linked by complex conjugation. At finite chemical potential this relation is lost and the effective potential depends on the two independent variables Φ and $\bar{\Phi}$. Extensions to finite μ_B have therefore to be carefully evaluated. Moreover, the flavor and density dependence of the pure Yang-Mills potential has not been explored as yet. We will show that it is possible to extract the qualitative behavior in the fully coupled system by perturbative arguments, as well as physical consistency arguments.

The outline of the paper is as follows: in the next section we introduce the Polyakov loop variable and discuss its effective potential derived from lattice data. The Polyakov loop potential is then coupled to the quark-

meson model which defines the Polyakov–quark-meson model. The grand canonical thermodynamic potential of this model is derived in mean-field approximation, and the choice of model parameters is discussed. Sec. III is devoted to thermodynamical applications, in particular we evaluate the pressure, quark number density and quark number susceptibility. Moreover, the phase structure, i.e. the chiral and confinement-deconfinement phase transition is explored. Subsequently, the influence of the Polyakov loop potential on the thermodynamics is investigated and in Sec. IV concluding remarks are drawn.

II. POLYAKOV–QUARK-MESON MODEL

A. Polyakov loop potential

A key observable in QCD at finite temperature is the Polyakov loop. Its expectation value serves as an order parameter for confinement in the heavy-quark limit. The Polyakov loop operator is a Wilson loop in the temporal direction and reads

$$\mathcal{P}(\vec{x}) = \mathcal{P} \exp \left(i \int_0^\beta d\tau A_0(\vec{x}, \tau) \right), \quad (2.1)$$

where \mathcal{P} stands for path-ordering and $A_0(\vec{x}, \tau)$ is the temporal component of the Euclidean gauge field A_μ [27, 28, 29, 30]. The color trace of (2.1) in the fundamental representation $\text{tr}_c \mathcal{P}(\vec{x})$ is the creation operator of a static quark at spatial position \vec{x} . Periodic boundary conditions ensure gauge invariance of Eq. (2.4) up to center elements. This goes hand in hand with the fact that the temporal or Weyl gauge $A_0 = 0$ cannot be achieved for periodic boundary conditions. Its physical interpretation is best seen in Polyakov gauge, where the temporal component of the gauge field is time-independent, $A_0(\vec{x}, \tau) = A_0^c(\vec{x})$, and is in the Cartan sub-algebra (see e.g. [31, 32, 33, 34]). Hence, within this gauge the Polyakov loop operator simplifies to

$$\mathcal{P}(\vec{x}) = \exp(i\beta A_0^c(\vec{x})), \quad (2.2)$$

with $A_0^c(\vec{x}) = A_0^{(3)}(\vec{x})\tau_3 + A_0^{(8)}(\vec{x})\tau_8$. This results in a simple relation between the Polyakov loop and the temporal component of the gauge field,

$$A_0^c(\vec{x}) = -i(\partial_\beta \mathcal{P}(\vec{x})) \mathcal{P}^\dagger(\vec{x}). \quad (2.3)$$

The normalized Polyakov loop variable $\Phi(\vec{x})$ and its hermitian (charge) conjugate $\bar{\Phi}(\vec{x})$ are defined as the

thermal expectation value of the color trace of the Polyakov loop operator (2.1)

$$\Phi(\vec{x}) = \frac{1}{N_c} \langle \text{tr}_c \mathcal{P}(\vec{x}) \rangle_\beta, \quad \bar{\Phi}(\vec{x}) = \frac{1}{N_c} \langle \text{tr}_c \mathcal{P}^\dagger(\vec{x}) \rangle_\beta. \quad (2.4)$$

We emphasize again that the traces are taken in the fundamental representation. $\Phi(\vec{x})$, $\bar{\Phi}(\vec{x})$ are complex scalar fields. Their mean values, i.e. the solution of the quantum equations of motion, are related to the free energy of a static, infinitely heavy test quark (antiquark) at spatial position \vec{x} . The order parameter $\Phi(\vec{x})$ vanishes in the confined phase where the free energy of a single heavy quark diverges. In the deconfined phase it takes a finite value. The correlation function of two Polyakov loop variables is related to the free energy $F_{q\bar{q}}$ of two color sources q and \bar{q} with spatial separation $\vec{r} = \vec{x} - \vec{y}$ as

$$\frac{1}{N_c^2} \langle \text{tr}_c \mathcal{P}(\vec{x}) \text{tr}_c \mathcal{P}^\dagger(\vec{y}) \rangle_\beta = e^{-\beta F_{q\bar{q}}(\vec{r})}. \quad (2.5)$$

The dependence on \vec{r} allows one to extract the string tension. The cluster decomposition property (locality) enforces that for infinite distance the correlation between a quark and anti-quark vanishes and we arrive at

$$\frac{1}{N_c^2} \langle \text{tr}_c \mathcal{P}(\vec{x}) \text{tr}_c \mathcal{P}^\dagger(\vec{y}) \rangle_\beta \rightarrow \Phi(\vec{x}) \bar{\Phi}(\vec{y}). \quad (2.6)$$

These properties provide the Polyakov criterion of confinement at finite temperature. It is linked to the center Z_{N_c} symmetry of the $SU(N_c)$ gauge group: a gauge transformation that is periodic up to a center element, leads to

$$\Phi \rightarrow z\Phi, \quad z \in Z_{N_c}. \quad (2.7)$$

Thus, the confining phase is center symmetric, whereas in the deconfined phase center symmetry is spontaneously broken.

In summary, the confinement-deconfinement phase transition is characterized by the mean value $\Phi = 0$ in the confined phase and a finite non-zero value in the deconfined phase. In the presence of dynamical quarks, the free energy of a quark-antiquark pair does not diverge anymore, and the order parameter is always non-vanishing. For finite quark chemical potential the free energies of quarks and antiquarks are different. Since Φ is related to the free energy of quarks and the hermitian (charge) conjugate $\bar{\Phi}$ to that of antiquarks, their modulus in general differs, i.e. $\bar{\Phi} \neq \Phi^\dagger$. In pure Yang-Mills theory the mean values Φ , $\bar{\Phi}$ are given by the minima of the effective Polyakov loop potential $\mathcal{U}(\Phi, \bar{\Phi})$. It can be constructed

from lattice data for the expectation values Φ , $\bar{\Phi}$ [10]. Here we use a polynomial expansion in Φ , $\bar{\Phi}$ up to quartic terms. This leads to an effective potential \mathcal{U} in terms of the moduli $|\Phi|$ and $|\bar{\Phi}|$, the product $\Phi\bar{\Phi}$, and in Φ^3 , $\bar{\Phi}^3$ related to the Z_3 symmetry. The $U(1)$ -symmetric part of \mathcal{U} is a Ginzburg-Landau type potential.

In pure Yang-Mills we can restrict ourselves to fields with the same modulus, $|\Phi| = |\bar{\Phi}|$. With this additional constraint we have $\Phi\bar{\Phi} = |\bar{\Phi}|^2$ and we can drop one of the $U(1)$ -invariants in the expansion. This has been used in Ref. [10] where the potential is only expanded in $\Phi\bar{\Phi}$, Φ^3 and $\bar{\Phi}^3$. Alternatively one can use the moduli and drop the $\Phi\bar{\Phi}$ -term. We conclude that the general effective potential in this approximation reads as

$$\begin{aligned} \frac{\mathcal{U}(\Phi, \bar{\Phi})}{T^4} = & -\frac{b_2}{4} (|\Phi|^2 + |\bar{\Phi}|^2) \\ & -\frac{b_3}{6} (\Phi^3 + \bar{\Phi}^3) + \frac{b_4}{16} (|\Phi|^2 + |\bar{\Phi}|^2)^2. \end{aligned} \quad (2.8)$$

The expansion coefficients are fixed to reproduce thermodynamic lattice results for the pure YM sector as in Refs. [18, 19, 35, 36, 37, 38]. This leads to temperature-independent coefficients $b_3 = 0.75$ and $b_4 = 7.5$, and a temperature-dependent one b_2 with

$$b_2(T) = a_0 + a_1 \left(\frac{T_0}{T}\right) + a_2 \left(\frac{T_0}{T}\right)^2 + a_3 \left(\frac{T_0}{T}\right)^3 \quad (2.9)$$

where $a_0 = 6.75$, $a_1 = -1.95$, $a_2 = 2.625$, $a_3 = -7.44$, $b_3 = 0.75$ and $b_4 = 7.5$. The effective potential (2.8) can be augmented by logarithmic terms, see e.g. Ref. [39]. This will be discussed in Sec. II D.

The potential (2.8) with the above parameters has a first-order phase transition at the critical temperature $T_0 = 270$ MeV.

B. Coupling to the quark-meson sector

The hadronic properties of low-energy QCD with light flavors are effectively incorporated by a chiral quark-meson model. Here the local $SU(N_c)$ gauge invariance of the underlying QCD is replaced by a global symmetry in the original quark-meson model which results in the loss of the confinement property. The QM model shows a chiral phase transition at realistic temperatures e.g. [4, 41]. In the limit of massless quarks the order parameter of the chiral phase transition is the quark condensate $\langle \bar{q}q \rangle$. For realistic up- and down quark masses chiral symmetry is broken spontaneously and also explicitly in the vacuum

resulting in a finite chiral condensate $\langle \bar{q}q \rangle$. Due to the lack of confinement in this model single quark states are already excited at low temperatures in the chirally broken phase, see e.g. [40] resulting in an unrealistic EoS near the phase transition. Since the constituent quark masses are much larger than that of the pion the meson dynamics dominates at low temperatures and the predictions from chiral perturbation theory are reproduced.

By combining the Polyakov loop model with the QM model chiral as well as confining properties of QCD are included. This promising approach has been put forward in [13, 14, 15, 16, 18, 42, 43, 44, 45] and significantly improved the EoS near the phase boundary. The integration over the gluonic degrees of freedom in the presence of a homogeneous background for the temporal component A_0 yields the Polyakov loop potential and the mesonic terms of the chiral QM model. Thus, the dynamical quark sector of QCD is included by integrating out the quarks in the presence of mean background fields. This finally leads to a coupled Polyakov–quark–meson model with an interaction potential between quarks, mesons and the Polyakov loop variables Φ , $\bar{\Phi}$. To leading loop order this potential is provided by the Dirac determinant in the presence of the mean fields.

The generalized Lagrangian of the linear QM model for $N_f = 2$ light quarks $q = (u, d)$ and $N_c = 3$ color degrees of freedom coupled to a spatially constant temporal background gauge field reads

$$\mathcal{L} = \bar{q}(i\not{D} - g(\sigma + i\gamma_5\vec{\tau}\vec{\pi}))q + \frac{1}{2}(\partial_\mu\sigma)^2 + \frac{1}{2}(\partial_\mu\vec{\pi})^2 - U(\sigma, \vec{\pi}) - \mathcal{U}(\Phi, \bar{\Phi}), \quad (2.10)$$

where the purely mesonic potential is defined as

$$U(\sigma, \vec{\pi}) = \frac{\lambda}{4}(\sigma^2 + \vec{\pi}^2 - v^2)^2 - c\sigma. \quad (2.11)$$

The isoscalar-scalar σ field and the three isovector-pseudoscalar pion fields $\vec{\pi}$ together form a chiral vector field $\vec{\phi}$. Without the explicit symmetry breaking term c in the mesonic potential the Lagrangian is invariant under global chiral $SU(2)_L \times SU(2)_R$ rotations. The covariant Dirac operator $D_\mu = \partial_\mu - iA_\mu$ in (2.10) reads

$$\not{D}(\Phi) = \gamma_\mu\partial_\mu - i\gamma_0A_0(\Phi). \quad (2.12)$$

The spatial components of the gauge fields have vanishing background i.e. $A_\mu = \delta_{\mu 0}A_0$.

C. Polyakov loop potential parameters

In the presence of dynamical quarks, the running coupling α is changed due to fermionic contributions. In our approximation to the Polyakov loop potential this only leads to a modification of the expansion coefficient b_2 , Eq. (2.9). The size of this effect can be estimated within perturbation theory, see e.g. [46, 47, 48, 49, 50]. At zero temperature it leads to an N_f -dependent decrease of Λ_{QCD} , which translates into an N_f -dependent decrease of the critical temperature T_0 at finite temperature. The two-loop β -function of QCD with massless quarks is given by

$$\beta(\alpha) = -b\alpha^2 - c\alpha^3, \quad (2.13)$$

with the coefficients

$$b = \frac{1}{6\pi}(11N_c - 2N_f), \quad (2.14)$$

$$c = \frac{1}{24\pi^2} \left(34N_c^2 - 10N_cN_f - 3\frac{N_c^2 - 1}{N_c}N_f \right). \quad (2.15)$$

Here, we have assumed a RG scheme that minimizes (part of) the higher-order effects. This is an appropriate scheme for our mean-field analysis. At leading order the corresponding gauge coupling is given by

$$\alpha(p) = \frac{\alpha_0}{1 + \alpha_0 b \ln(p/\Lambda)} + O(\alpha_0^2), \quad (2.16)$$

with $\alpha_0 = \alpha(\Lambda)$ at some UV-scale Λ , and $\Lambda_{\text{QCD}} = \Lambda \exp(-1/(\alpha_0 b))$. At $p = \Lambda_{\text{QCD}}$ the coupling (2.16) exhibits a Landau pole. At finite temperature the relation (2.16) allows us to determine the N_f -dependence of the critical temperature $T_0(N_f)$. For $N_f = 0$ it is given by $T_0 = 270$ MeV which corresponds to fixing the coupling α_0 at the τ -scale $T_\tau = 1.770$ GeV and a running coupling of $\alpha_0 = 0.304$ accordingly. If one keeps the coupling α_0 at T_τ fixed, this identification yields the relation

$$T_0(N_f) = T_\tau e^{-1/(\alpha_0 b)}, \quad (2.17)$$

and Table I for the N_f -dependent critical temperature T_0 in the Polyakov loop potential for massless flavors:

N_f	0	1	2	2 + 1	3
T_0 [MeV]	270	240	208	187	178

TABLE I: Critical Polyakov loop temperature T_0 for N_f massless flavors.

Massive flavors lead to suppression factors of the order $T_0^2/(T_0^2 + m^2)$ in the β -function. For 2 + 1 flavors and

a current strange quark mass $m_s \approx 150$ MeV we obtain $T_0(2+1) = 187$ MeV. We remark that the estimates for $T_0(N_f)$ have an uncertainty at least of the order ± 30 MeV. This uncertainty comes from the perturbative one-loop nature of the estimate and the poor accounting for the temperature effects. For example, with the two loop coefficient (2.15) and concentrating on $N_f = 2$ as studied in the present work we are led to $T_0(2) = 192$ MeV. Fortunately, the results only show a mild T_0 dependence.

Finally, we argue that there are no double counting effects due to the inclusion of the Dirac determinant in the PQM and the independent adjustment of the Polyakov loop model parameters: the Polyakov loop potential parameters, in particular b_2 , Eq. (2.9), genuinely depend on the running coupling, which is changed in the presence of quarks. This effect is modeled by changing $T_0 \rightarrow T_0(N_f)$ as defined in Eq. (2.17). The direct contributions to the Polyakov loop potential which originate from the fermionic determinant $\Omega_{\bar{q}q}$, Eq. (3.24), are not governed by this redefinition, and have to be added separately.

D. Non-vanishing chemical potential

A further intricacy concerns the Polyakov loop potential at finite chemical potential [51, 52]. Then the constraint $\bar{\Phi} = \Phi^\dagger$ ceases to be valid, and the extension of Eq. (2.8) to finite μ is not unique anymore. For further details see e.g. Refs. [53, 54]. The leading μ -dependence of the full potential stems from the Dirac determinant, and we assume that the $\Phi, \bar{\Phi}$ -symmetric form of the potential (2.8) persists at finite μ . Then the only additional μ dependence originates from a possible μ dependence of the model parameters. This approximation certainly is valid for small chemical potential where the μ dependence is rather small. The remaining ambiguity concerns possible $\Phi\bar{\Phi}$ -terms, that can be incorporated into the potential (2.8) by the replacement

$$\frac{1}{2}(|\Phi|^2 + |\bar{\Phi}|^2) \rightarrow \frac{1}{2}\theta(|\Phi|^2 + |\bar{\Phi}|^2) + (1-\theta)\Phi\bar{\Phi}. \quad (2.18)$$

Eq. (2.18) leaves the potential unchanged for $\mu = 0$, that is $\bar{\Phi} = \Phi^\dagger$. For positive θ the potential has unstable directions, e.g. for vanishing Φ or $\bar{\Phi}$, and large $\bar{\Phi}$, Φ respectively. Hence the choice $\theta = 0$ possibly leads to negative susceptibilities. In Refs. [18, 20] this choice has been used, and the computed susceptibilities are not positive anymore [20]. This problem has been cured in Refs. [20, 39, 51] by augmenting the Polyakov loop potential with logarithmic terms. Effectively, this amounts to

changing the model parameters in the polynomial ansatz used in these works. For $\theta \neq 0$ these logarithmic terms are not necessary, due to lack of unstable directions. Furthermore, a weak total μ dependence as well as the validity of the mean-field analysis would hint at the preferred choice $\theta = 1$. However, for this choice the expectation value of $(\bar{\Phi} - \Phi)$ has the wrong sign, even though other observables show a mild θ -dependence. Clearly, this structure is related to the present mean-field approximation. It should be possible to overcome this parameter dependence in a fully non-perturbative setting. Here, we shall show results for the choice $\theta = 0$.

In a final step we implement a μ -dependent running coupling in the b_2 coefficient, analogous to the N_f -dependence discussed above. Indeed, one can argue that this is a minimal necessary generalization: without a μ -dependent b_2 the confinement-deconfinement phase-transition has a higher critical temperature than the chiral phase transition at vanishing chemical potential. This is an unphysical scenario because QCD with dynamical massless quarks in the chirally restored phase cannot be confining since the string breaking scale would be zero.

As for the N_f -dependence we resort to perturbative estimates. To begin with we simply allow for an additional μ -dependent term in the one-loop coefficient b ,

$$b(\mu) = \frac{1}{6\pi}(11N_c - 2N_f) - b_\mu \frac{\mu^2}{T_\tau^2}. \quad (2.19)$$

This specific simple choice of the μ -dependent part can be motivated by using HDL/HTL results on the effective charge [55]

$$\alpha(p, T, \mu) = \frac{\alpha(p)}{1 + m_D^2/p^2}, \quad (2.20)$$

with the perturbative Debye mass $m_D^2 = (N_c/3 + N_f/6)g^2T^2 + N_f/(2\pi^2)g^2\mu^2$. The μ -derivative of the modified coupling, $\mu\partial_\mu\alpha = b_\mu\mu^2/p^2$, can be related to a momentum derivative $p\partial_p\alpha = -b(p, \mu)\alpha^2$. Within the present simple approach based on a μ -dependence only valid in the perturbative regime we estimate the momentum-dependent coefficient $b(p, \mu)$ by $b(\mu) = b(\gamma T_\tau, \mu)$ at an (average) momentum scale γT_τ with $\gamma \leq 1$.

The coefficient b_μ can be fixed such that the chiral transition temperature and the confinement-deconfinement transition agree at some non-vanishing μ . Interestingly, it turns out that then the transition temperatures agree for all μ 's. The related value of b_μ is provided by $\gamma \simeq 1/4$

and

$$b_\mu \simeq \frac{16}{\pi} N_f. \quad (2.21)$$

Inserting the μ -dependent coefficient $b(\mu)$ into Eq. (2.17) then leads to an additional μ -dependent T_0 ,

$$T_0(\mu, N_f) = T_\tau e^{-1/(\alpha_0 b(\mu))}. \quad (2.22)$$

Eq. (2.22) with (2.21) should be viewed as a rough estimate of the μ -dependence of T_0 . We emphasise again that this simple estimate leads to coinciding phase boundary lines for the chiral and confinement-deconfinement transition, see Sec. III. For more quantitative results the non-perturbative running of the coupling in the presence of finite temperature and quark density has to be considered. This can be incorporated in a self-consistent RG-setting. Moreover, one has to resolve the uncertainties, discussed at the beginning of this section, concerning the form of the effective potential at finite μ .

Here we will present a comparison of the phase diagram with and without μ -dependent T_0 in Fig. 6. For the other results the additional μ -dependence is taken into account.

III. APPLICATIONS

The PQM model is defined by the Lagrangian (2.10) with the Polyakov loop potential Eq. (2.8). The dependence of the coefficient b_2 Eq. (2.9) on the N_f -dependent or (N_f, μ) -dependent running coupling α is governed by Eq. (2.17) and (2.22) respectively. This defines the starting point for an investigation of the phase structure and bulk thermodynamics of the PQM model. The thermodynamics is characterized by the grand canonical potential which is analyzed in mean-field approximation.

A. Grand canonical potential

The grand canonical potential in a spatially uniform system is determined as the logarithm of the partition function, which in our case is a path-integral over the meson and quark/antiquark fields including the Polyakov loop. We confine ourselves to the $SU(2)_f$ -symmetric case and set $\mu \equiv \mu_u = \mu_d$. This is a good approximation to the realistic case since flavor mixing in the vector channel is small. Integrating over the fermions by using the Nambu-Gor'kov formalism and introducing averaged meson fields yields the grand canonical potential

$$\Omega = \mathcal{U}(\Phi, \bar{\Phi}) + U(\sigma) + \Omega_{\bar{q}q}(\Phi, \bar{\Phi}, \sigma) \quad (3.23)$$

with the quark/antiquark contribution

$$\Omega_{\bar{q}q} = -2N_f T \int \frac{d^3 p}{(2\pi)^3} \text{tr}_c \left\{ \ln(1 + \mathcal{P} e^{-(E_p - \mu)/T}) + \ln(1 + \mathcal{P}^\dagger e^{-(E_p + \mu)/T}) \right\} \quad (3.24)$$

and the purely mesonic potential

$$U(\sigma) = \frac{\lambda}{4} (\sigma^2 - v^2)^2 - c\sigma. \quad (3.25)$$

The divergent vacuum part in the quark/anti-quark contribution is absorbed in the renormalization which is done in the vacuum. The quark/antiquark single-quasiparticle energy is given by

$$E_p = \sqrt{\vec{p}^2 + m_q^2} \quad (3.26)$$

with the constituent quark mass $m_q = g\sigma$. The remaining color trace in the quark/antiquark contribution (3.24) is evaluated by using the identity $\text{Tr} \ln A = \ln \det A$ and yields

$$\Omega_{\bar{q}q} = -2N_f T \int \frac{d^3 p}{(2\pi)^3} \quad (3.27)$$

$$\left\{ \ln \left[1 + 3(\Phi + \bar{\Phi} e^{-(E_p - \mu)/T}) e^{-(E_p - \mu)/T} + e^{-3(E_p - \mu)/T} \right] + \ln \left[1 + 3(\bar{\Phi} + \Phi e^{-(E_p + \mu)/T}) e^{-(E_p + \mu)/T} + e^{-3(E_p + \mu)/T} \right] \right\}.$$

Note, that no ultraviolet cutoff is necessary because the PQM model is renormalizable in contrast to the PNJL model (see e.g. [18, 19]).

The equations of motion are obtained by minimizing the thermodynamic potential (3.23) w.r.t. the three constant mean fields σ , Φ and $\bar{\Phi}$:

$$\frac{\partial \Omega}{\partial \sigma} = \frac{\partial \Omega}{\partial \Phi} = \frac{\partial \Omega}{\partial \bar{\Phi}} \Big|_{\sigma=\langle\sigma\rangle, \Phi=\langle\Phi\rangle, \bar{\Phi}=\langle\bar{\Phi}\rangle} = 0. \quad (3.28)$$

The solutions of these coupled equations determine the behavior of the chiral order parameter $\langle\sigma\rangle$ and the Polyakov loop expectation values $\langle\Phi\rangle$ and $\langle\bar{\Phi}\rangle$ as a function of T and μ .

B. Quark-meson parameters

The four parameters of the QM model, i.e. g , λ , v and c , are chosen such that chiral symmetry is spontaneously broken in the vacuum and the σ -field develops a finite expectation value $\langle\sigma\rangle \equiv f_\pi$, where $f_\pi = 93$ MeV is set to

the pion decay constant. Due to the pseudoscalar character of the pions the corresponding expectation values vanish, $\langle \bar{\pi} \rangle = 0$.

The Yukawa coupling constant g is fixed by the constituent quark mass in the vacuum $g = m_q/f_\pi$. Using the partially conserved axial vector current (PCAC) relation the explicit symmetry breaking parameter c is determined by $c = m_\pi^2 f_\pi$, where m_π is the pion mass. The quartic coupling constant λ is given by the sigma mass m_σ via the relation $\lambda = (m_\sigma^2 - m_\pi^2)/(2f_\pi^2)$. Finally, the parameter v^2 is found by minimizing the potential in radial direction, yielding $v^2 = \langle \sigma \rangle^2 - c/(\lambda \langle \sigma \rangle)$. For the ground state where $\langle \sigma \rangle = f_\pi$ this expression can be rewritten as $v^2 = f_\pi^2 - m_\pi^2/\lambda$. It is positive in the Nambu-Goldstone phase.

In the vacuum we fix the model parameters to $m_\pi = 138$ MeV, $m_\sigma = 600$ MeV, $f_\pi = 93$ MeV and $m_q = 300$ MeV which result in $c \sim 1.77 \cdot 10^6$ MeV³, $v \sim 87.6$ MeV, $\lambda \sim 19.7$ and $g \sim 3.2$.

C. Phase structure

The phase structure of the PQM model is determined by the behavior of the order parameters σ , Φ and $\bar{\Phi}$ and of the grand canonical potential as a function of temperature and quark chemical potential. All numerical results have been obtained for $N_f = 2$. Then $T_0 = 208$ MeV in agreement with Tab. I. This value is different from that taken in Ref. [18, 56] where $T_0 = 270$ MeV, the value of $N_f = 0$. In these works $T_0 = 210$ MeV has been fixed in order to compare with lattice results. The N_f -dependence suggested in the present work offers a qualitative explanation for this choice.

In Fig. 1 the temperature dependence of the chiral condensate $\langle \bar{q}q \rangle$ and the Polyakov loop expectation value Φ , see Eq. (2.4), at $\mu = 0$ is shown in relative units.

For vanishing chemical potential we have $\bar{\Phi} = \Phi$ as already discussed. For $T \rightarrow \infty$ we find $\Phi \simeq 1.11$. Since the properly normalized expectation value $\bar{\Phi}$ tends towards unity we have normalized the mean fields accordingly. For temperatures at about 200-300 MeV the normalized $\bar{\Phi}$ has a μ -dependent maximum and decreases for larger temperatures towards one, see Fig. 2. This is in qualitative agreement with perturbation theory which predicts an increasing $\bar{\Phi}$ within an expansion around vanishing gauge fields, e.g. [57, 58].

At $\mu = 0$ we find a chiral crossover temperature

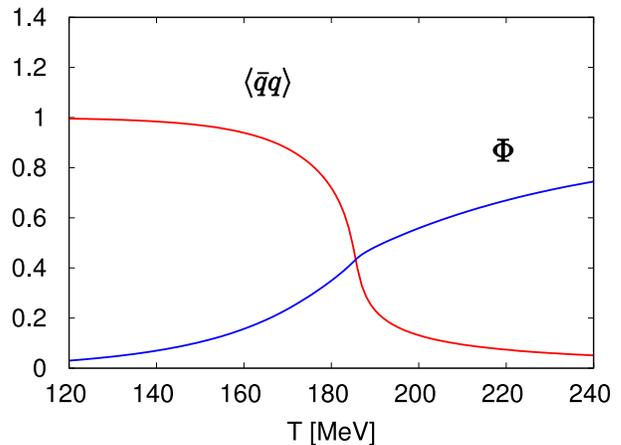


FIG. 1: The normalized chiral condensate $\langle \bar{q}q \rangle$ and the Polyakov loop Φ as a function of temperature for $\mu = 0$. A chiral crossover is found at $T \sim 180$ MeV and a deconfinement crossover at a similar temperature.

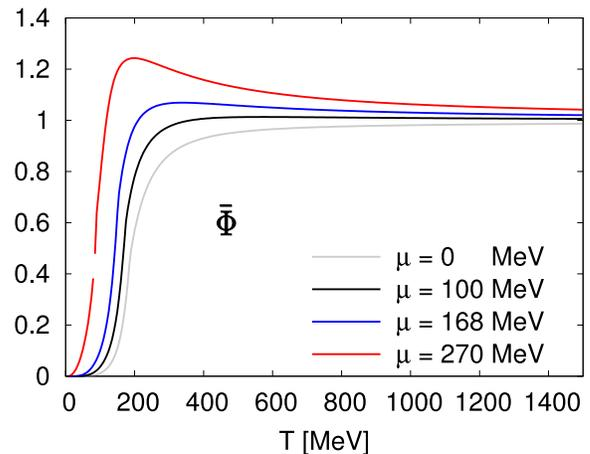


FIG. 2: The normalized Polyakov loop variable $\bar{\Phi}$ for large temperatures for several chemical potentials μ .

$T_c = 184$ MeV with an error of $\sim \pm 14$ MeV originating in the error estimate ± 30 MeV for T_0 . For example, using the two-loop running of the coupling (2.15), and hence $T_0(N_f) = 192$ MeV we are led to $T_c \sim 177$ MeV. In the presence of dynamical quarks the Polyakov loop shows also a crossover at the same pseudo-critical temperature. This can be read off from the peak position of $\partial \langle \bar{q}q \rangle / \partial T$ and $\partial \Phi / \partial T$. In Fig. 3 these quantities are shown as function of the temperature.

In two-flavor lattice simulations extrapolated to the chiral limit a pseudo-critical temperature $T_c = 173 \pm 8$ MeV is found using improved staggered fermions [1]. Recently, a recalculation of the transition temperature with staggered fermions for two light and one heavier quark

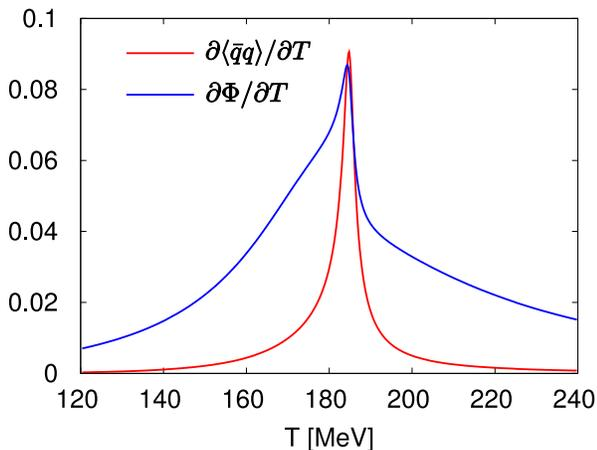


FIG. 3: The temperature dependence of $\partial\langle\bar{q}q\rangle/\partial T$ and $\partial\Phi/\partial T$ for $\mu = 0$. The Polyakov variable is scaled by a factor of 5.

mass close to their physical values yields a $T_c = 192 \pm 7$ MeV using the Sommer parameter r_0 for the continuum extrapolation [59]. This result has to be contrasted with another recent lattice analysis with staggered fermions but using four different sets of lattice sizes $N_\tau = 4, 6, 8$ and 10 to perform the continuum extrapolation [60]. From the same physical observable this group finds a critical temperature $T_c = 151 \pm 3$ MeV. Functional RG studies yield a critical value of $T_c = 172_{-34}^{+40}$ MeV [49, 50], where the error originates in an estimate of the uncertainty similar to the considerations put forward here. On the other hand, using the same parameters for the quark-meson model without the Polyakov loop modifications a crossover temperature of $T_c \sim 150$ MeV emerges [61]. This situation calls for refined studies both on the lattice as well as within functional methods to resolve the apparent quantitative inaccuracies.

For finite μ the degeneracy of Φ and $\bar{\Phi}$ disappears. The corresponding order parameters as function of temperature for several chemical potentials are collected in Figs. 4 and 5. For finite μ the Polyakov loop $\bar{\Phi}$ is always larger than Φ . It has a positive slope $\partial\bar{\Phi}/\partial\mu > 0$ for all temperatures, and peaks at some high temperature, see Fig. 2. Both, Φ and $\bar{\Phi}$ tend towards one for $T \rightarrow \infty$.

Above a critical chemical potential $\mu_c = 168$ MeV all order parameters jump at the same temperature which signals a first-order phase transition. The critical end point (CEP) is found at $(T_c, \mu_c) = (150, 168)$ MeV. The corresponding chiral phase diagram obtained for a μ -independent $T_0(N_f)$, (2.17), is shown in Fig. 6 (upper lines). At the critical point the chiral first-order transition line terminates and the transition becomes second-

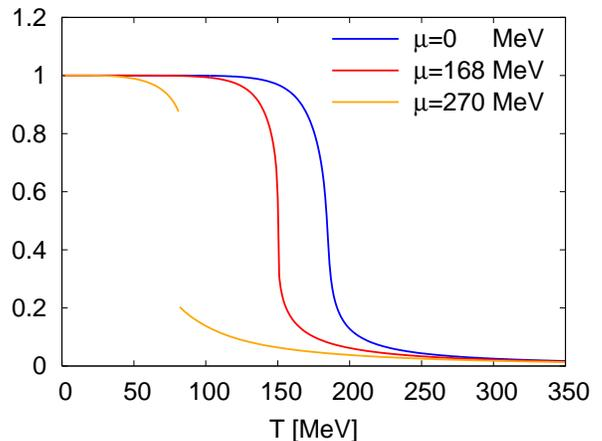


FIG. 4: The normalized chiral quark condensate $\langle\sigma\rangle$ as a function of temperature for three different chemical potentials $\mu = 0, 168, 270$ MeV. For $\mu = 270$ MeV a first-order transition is found at $T_c \sim 81$ MeV.

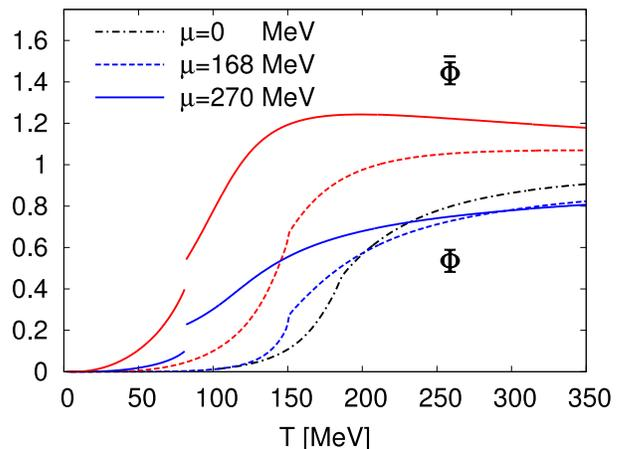


FIG. 5: Same as Fig. 4 for the normalized Polyakov loops $\bar{\Phi}$ and Φ .

order, which induces a divergent quark number susceptibility. Lattice simulations are not conclusive concerning the existence and location of the critical point [1, 62, 67].

There are indications from lattice simulations at finite chemical potential that deconfinement and chiral symmetry restoration appear along the same critical line in the phase diagram. For the PQM model and μ -independent $T_0(N_f)$ the coincidence of deconfinement and chiral transition at $\mu = 0$ disappears for finite μ . The deconfinement temperature is larger than the corresponding chiral transition temperature. This is an unphysical scenario because the deconfinement temperature should be smaller or equal to the chiral transition temperature. When resorting to the μ -dependent $T_0(\mu, N_f)$, (2.22), we find coinciding transition lines for the entire phase diagram

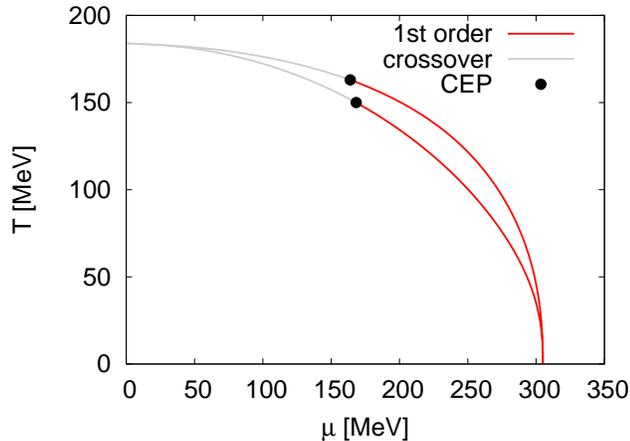


FIG. 6: Chiral phase diagrams for the PQM model. Upper lines for a μ -independent Polyakov loop potential and lower lines with μ -dependent corrections. The CEP's are approximately located at $(T_c, \mu_c) = (163, 164)$ MeV (upper case) and at $(150, 168)$ MeV (lower case).

within an accuracy of ± 5 MeV. For this case the unique transition line lies slightly below the chiral one for the μ -independent choice $T_0(N_f)$. This is shown in Fig. 6.

D. Thermodynamic observables

In order to investigate the influence of the Polyakov loop on the equilibrium thermodynamics we calculate several thermodynamic observables. All information of the system is contained in the grand canonical potential which is given by Ω in (3.23) evaluated at the mean-field level.

We begin our analysis with the pressure of the system p . It is defined as the negative of the grand canonical potential and is normalized to vanish at $T = \mu = 0$. In Fig. 7 the pressure divided by the QCD Stefan-Boltzmann (SB) limit is shown as function of the temperature for three different quark chemical potentials. The values of the chemical potentials are chosen such that one curve runs through the critical end point (CEP) ($\mu_c = 168$ MeV) and another curve through a first-order phase transition ($\mu = 270$ MeV). The QCD pressure in the SB limit for N_f massless quarks and $(N_c^2 - 1)$ massless gluons, relevant for the deconfined phase, is given by

$$\frac{p_{\text{SB}}}{T^4} = (N_c^2 - 1) \frac{\pi^2}{45} + N_c N_f \left[\frac{7\pi^2}{180} + \frac{1}{6} \left(\frac{\mu}{T} \right)^2 + \frac{1}{12\pi^2} \left(\frac{\mu}{T} \right)^4 \right]. \quad (3.29)$$

where the first term denotes the gluonic contribution

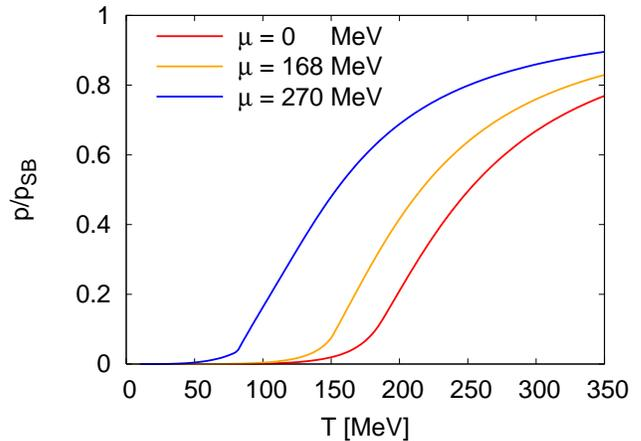


FIG. 7: Scaled pressure p/p_{SB} for three different quark chemical potentials, $\mu = 0, 168, 270$ MeV. $T_c(\mu = 0) = 184$ MeV.

and the rest involves the fermions. The pressure is suppressed in the confined phase and starts to rise when deconfinement sets in. For all T and μ the pressure p/T^4 stays below the QCD SB limit, a feature that is also observed in lattice calculations and other non-perturbative approaches. For vanishing chemical potential the pressure is a smooth function of the temperature consistent with a crossover transition. At temperatures of twice the critical temperature the pressure reaches approximately 80% of the SB limit. On the lattice two classes of data for the pressure obtained with a temporal extent $N_\tau = 4$ and $N_\tau = 6$ at $\mu = 0$ are currently available both of which are not extrapolated to the continuum [63, 64]. Our results are in agreement with lattice simulations with a temporal extent of $N_\tau = 6$ which is also closer to the continuum limit. This behavior is demonstrated in Fig. 8.

An increase of the chemical potential leads to an increase of the pressure as more quark degrees of freedom are active. For a certain chemical potential the crossover transition changes to a first-order phase transition. In this case the pressure has a kink at the transition point but still is a continuous function. The kink at $T \sim 100$ MeV for the $\mu = 270$ MeV curve is clearly visible Fig. 7.

At a first-order phase transition a finite latent heat builds up. This results in a jump of the entropy density s , which is defined as the negative derivative of the grand canonical potential with respect to the temperature. It is identical to the temperature derivative of the pressure. In Fig. 9 we show s divided by the corresponding QCD SB limit for the same chemical potentials as in the preceding figure. The low- and high-temperature behavior of this quantity can be understood in a similar fashion as

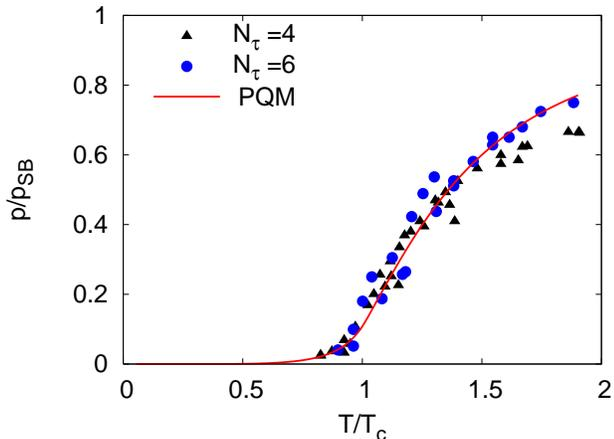


FIG. 8: Scaled pressure p/p_{SB} for $\mu = 0$. The PQM model prediction (solid line) is compared to lattice results for $N_\tau = 4$ and $N_\tau = 6$. Lattice data taken from Ref. [63].

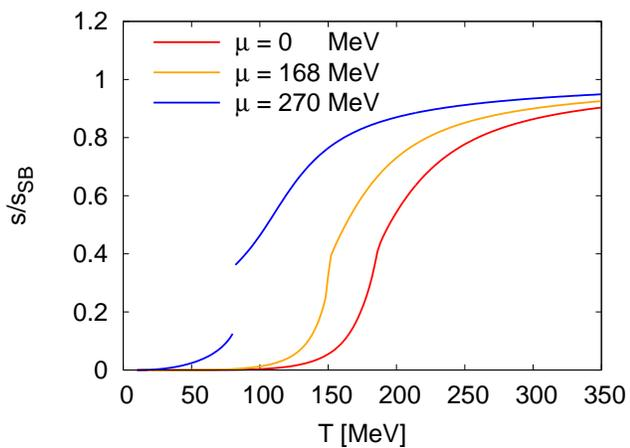


FIG. 9: Same as described in the legend to Fig. 7 for the scaled entropy s/s_{SB} .

those of the pressure. It is continuous in the vicinity of the crossover transition and reaches less than 40% of the SB limit around these temperatures. For chemical potential values larger than the critical one a finite latent heat emerges which further increases with the chemical potential.

Another quantity that is accessible in lattice QCD at finite chemical potential is the pressure difference Δp . It is defined as $\Delta p(T, \mu) = p(T, \mu) - p(T, \mu = 0)$ and is Taylor-expanded around $\mu = 0$ in powers of the dimensionless quantity μ/T on the lattice. Because odd derivatives of the free energy with respect to μ vanish only even powers appear in this expansion. In our model we have computed the pressure difference without referring to an expansion. In Fig. 10 the scaled pressure differ-

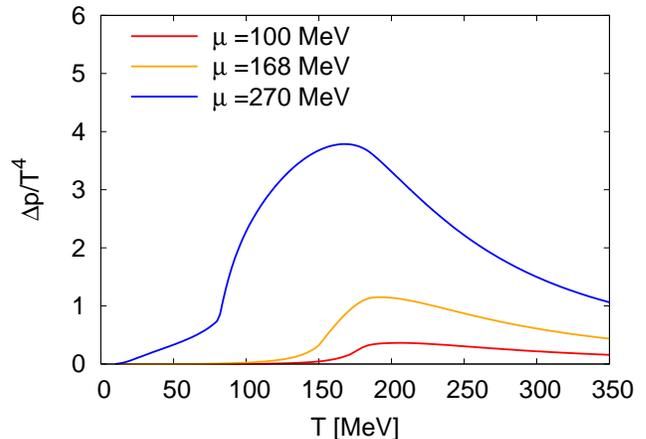


FIG. 10: Scaled pressure difference $\Delta p/T^4$ for three different chemical potentials. The curves correspond to $\mu = 100, 168, 270$ MeV from below.

ence $\Delta p(T, \mu)/T^4$ versus temperature for three chemical potential values is shown. The bottom curve corresponds to $\mu = 100$ MeV. It is always a continuous function and shows a kink at a first-order phase transition. Δp rises steeply across the chiral transition and peaks almost at the same temperature for all chemical potentials. For larger temperatures it decreases almost as $1/T^2$ which follows from the SB limit. Nevertheless, due to the T - and μ -dependent Polyakov fields slight deviations of the $1/T^2$ SB behavior are seen.

Another interesting observable is the net quark density. It is obtained from the thermodynamic potential via $n_q = -\partial\Omega(T, \mu)/\partial\mu$. The quark density, normalized to $1/T^3$, is displayed as a function of the temperature in Fig. 11 for three different chemical potentials $\mu = 100, 168$ and 270 MeV. In comparison to the pure quark-meson model without the Polyakov loop the quark density in the confined phase is much more suppressed when the interaction of quarks with the Polyakov loop is added [40, 61]. A similar effect is seen in the PNJL model [20]. Above the phase transition, the quark density of the pure quark-meson model approaches the Stefan-Boltzmann limit $n_q = N_f\mu(T^2 + (\mu/\pi)^2)$ immediately. With the Polyakov loop dynamics this behavior is changed drastically. The quark densities increase slightly above the corresponding SB limits and decrease again with growing temperature. For high temperatures the SB limit of the quark density is always reached from above. At a first-order phase transition n_q jumps and drops immediately after the transition for increasing temperatures.

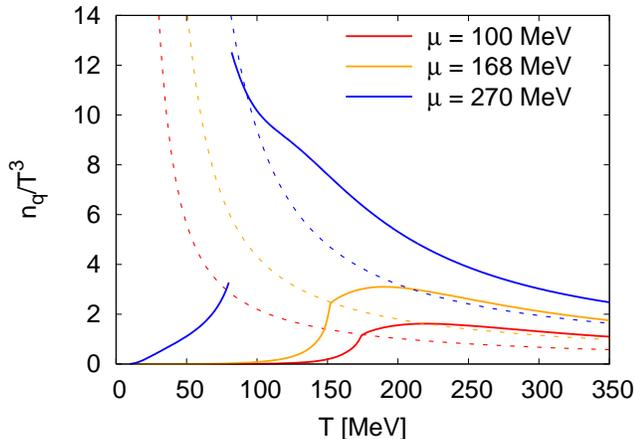


FIG. 11: Same as described in the legend to Fig. 10 for the quark number density n_q/T^3 . The dashed lines denote the corresponding Stefan-Boltzmann limits.

The quark number susceptibility measures the static response of the quark number density to an infinitesimal variation of the quark chemical potential and is given by $\chi_q = \partial n_q / \partial \mu$. It is shown in Fig. 12 as a function of temperature for several μ . This observable can be

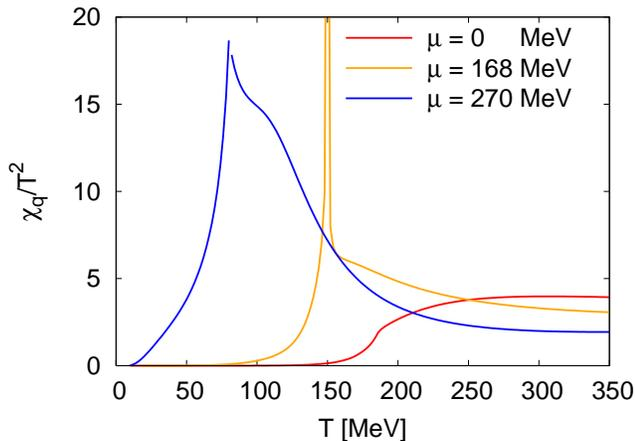


FIG. 12: The scaled chiral susceptibility χ_q/T^2 as a function of temperature for three different quark chemical potentials, $\mu = 0, 168, 270$ MeV.

used to verify the existence and location of the critical end point in the phase diagram. At a first-order phase transition this quantity has a discontinuity and only at a second-order critical end point it is divergent. Even for finite pion masses the critical point is of second-order and induces a divergent quark number susceptibility. This behavior is seen in Fig. 12. For $\mu = 168$ MeV, close to the critical chemical potential, χ_q diverges at the critical temperature.

The modifications caused by the quark-gluon interaction on the quark number susceptibility, are similar as those already discussed in the context of the quark number density. Compared to the pure quark-meson model χ_q is again more suppressed below the chiral phase transition. Above the transition χ_q lies above the corresponding SB limit $\chi_q/T^2 = N_f(1 + 3/\pi^2(\mu/T)^2)$. At high temperatures the SB limit (not shown in the figure) is again reached from above.

IV. CONCLUSION

In the present paper we have extended the $N_f = 2$ quark-meson model to include certain aspects of gluon dynamics via the Polyakov loop. This PQM model combines important symmetry aspects in the limit of infinitely heavy quarks with those of the light quark sector of nearly massless up- and down quarks. Within the mean-field approximation we have discussed the ensuing phase diagram of strongly interacting matter in the grand canonical ensemble, as was done previously in a similar extension of the NJL model [39, 51, 65]. One of the benefits is an improvement of the thermodynamical behavior of several bulk quantities such as pressure, entropy etc. when compared to lattice data. As a novelty we propose to include the N_f and μ dependence of the the running coupling α in the parameter of the Polyakov loop potential. A qualitative estimate is provided by the one loop β -function for the gauge coupling α as well as using the hard dense loop approximation. Then we are led to a N_f and μ dependent T_0 , the critical temperature of the Polyakov loop model, which decreases with increasing N_f and μ . These modifications already involve coinciding peaks in the temperature derivative of the Polyakov loop expectation value and the chiral condensate at $\mu = 0$, in agreement with the lattice findings of [66, 67]. Interestingly this coincidence of the deconfinement and chiral symmetry restoration persists at finite μ .

The findings of the present work provide a promising starting point for a functional RG study in the present model [26], and further extensions towards full QCD: in particular, we aim at removing the perturbative nature of the above estimates as well as allowing for a fully coupled PQM model. The last step consists of including the full gauge dynamics. This is particularly relevant for the important issue of the Polyakov loop potential at finite μ , being intimately related to the open question of the existence and location of the critical point in the QCD

phase diagram.

Acknowledgment

We thank R. Alkofer, B. Friman, H. Gies, R.D. Pisarski, C. Ratti, K. Redlich, S. Rößner, C. Sasaki,

I.O. Stamatescu, L. von Smekal and W. Weise for useful discussions, and the referee for useful comments.

-
- [1] F. Karsch, Lect. Notes Phys. **583**, 209 (2002).
 [2] J. Greensite, Prog. Part. Nucl. Phys. **51**, 1 (2003).
 [3] D. F. Litim and J. M. Pawłowski, [hep-th/9901063](#); J. Polonyi, Central Eur. J. Phys. **1**, 1 (2003); J. Berges, N. Tetradis and C. Wetterich, Phys. Rept. **363**, 223 (2002); J. M. Pawłowski, Annals Phys. doi: 10.1016/j.aop.2007.01.007 (2007); H. Gies, [hep-ph/0611146](#).
 [4] B.-J. Schaefer and J. Wambach, [hep-ph/0611191](#).
 [5] C. D. Roberts and S. M. Schmidt, Prog. Part. Nucl. Phys. **45**, S1 (2000); R. Alkofer and L. von Smekal, Phys. Rept. **353**, 281 (2001); C. S. Fischer, J. Phys. **G32**, R253 (2006).
 [6] N. Weiss, Phys. Rev. **D24**, 475 (1981).
 [7] M. Engelhardt and H. Reinhardt, Phys. Lett. **B430**, 161 (1998).
 [8] H. Gies, Phys. Rev. **D63**, 025013 (2001).
 [9] J. Braun, H. Gies, and J.M. Pawłowski, [arXiv:0708.2413 \[hep-th\]](#).
 [10] R. D. Pisarski, Phys. Rev. **D62**, 111501 (2000).
 [11] R. D. Pisarski, Phys. Rev. **D74**, 121703 (2006).
 [12] K. Fukushima and K. Ohta, J. Phys. **G26**, 1397 (2000).
 [13] K. Fukushima, Phys. Rev. **D68**, 045004 (2003).
 [14] K. Fukushima, Phys. Lett. **B591**, 277 (2004).
 [15] K. Fukushima, Ann. Phys. **304**, 72 (2003).
 [16] P. N. Meisinger, T. R. Miller, and M. C. Ogilvie, Nucl. Phys. Proc. Suppl. **119**, 511 (2003).
 [17] P. N. Meisinger, T. R. Miller, and M. C. Ogilvie, Nucl. Phys. Proc. Suppl. **129**, 563 (2004).
 [18] C. Ratti, M. A. Thaler, and W. Weise, Phys. Rev. **D73**, 014019 (2006).
 [19] C. Ratti and W. Weise, Phys. Lett. **D70**, 054013 (2004).
 [20] C. Sasaki, B. Friman, and K. Redlich, [hep-ph/0611147](#).
 [21] P. N. Meisinger and M. C. Ogilvie, Phys. Lett. **B379**, 163 (1996).
 [22] R. D. Pisarski and F. Wilczek, Phys. Rev. **D29**, 338 (1984).
 [23] A. Mocsy, F. Sannino, and K. Tuominen, Phys. Rev. Lett. **92**, 182302 (2004).
 [24] P. N. Meisinger, T. R. Miller, and M. C. Ogilvie, Phys. Rev. **D65**, 034009 (2002).
 [25] H. Gies and C. Wetterich, Phys. Rev. **D69**, 025001 (2004).
 [26] J. M. Pawłowski, B.-J. Schaefer, and J. Wambach, work in progress (2007).
 [27] A. M. Polyakov, Phys. Lett. **B72**, 477 (1978).
 [28] L. Susskind, Phys. Rev. **D20**, 2610 (1979).
 [29] C. Borgs and E. Seiler, Commun. Math. Phys. **91**, 329 (1983).
 [30] J. Kuti, J. Polonyi, and K. Szlachanyi, Phys. Lett. **B98**, 199 (1981).
 [31] H. Reinhardt, Nucl. Phys. **B503**, 505 (1997).
 [32] C. Ford, U. G. Mitreuter, J. M. Pawłowski, T. Tok, and A. Wipf, Annals Phys. **269**, 26 (1998).
 [33] C. Ford, T. Tok, and A. Wipf, Phys. Lett. **B456**, 155 (1999).
 [34] O. Jahn and F. Lenz, Phys. Rev. **D58**, 085006 (1998).
 [35] R. De Pietri, A. Feo, E. Seiler, and I.-O. Stamatescu, [POS LAT2005](#), 170 (2005).
 [36] T. Heinzl, T. Kaestner, and A. Wipf, Phys. Rev. **D72**, 065005 (2005).
 [37] P. de Forcrand and L. von Smekal, Phys. Rev. **D66**, 011504 (2002).
 [38] C. Wozar, T. Kaestner, A. Wipf, T. Heinzl, and B. Pozsgay, Phys. Rev. **D74**, 114501 (2006).
 [39] C. Ratti, S. Roessner, and W. Weise, [hep-ph/0701091](#).
 [40] B.-J. Schaefer and H.-J. Pirner, Nucl. Phys. **A660**, 439 (1999).
 [41] D.-U. Jungnickel and C. Wetterich, Phys. Rev. **D53**, 5142 (1996); J. Berges, D.-U. Jungnickel and C. Wetterich, Int. J. Mod. Phys. **A18**, 3189 (2003); N. Tetradis, Nucl. Phys. **A726**, 93 (2003).
 [42] E. Megias, E. Ruiz Arriola, and L. L. Salcedo, [PoS JHW2005](#), 025 (2006).
 [43] E. Megias, E. Ruiz Arriola, and L. L. Salcedo, Phys. Lett. **B563**, 173 (2003).
 [44] E. Megias, E. Ruiz Arriola, and L. L. Salcedo, Phys. Rev. **D74**, 065005 (2006).
 [45] E. Megias, E. Ruiz Arriola, and L. L. Salcedo, Phys. Rev. **D74**, 114014 (2006).
 [46] T. Banks and A. Zaks, Nucl. Phys. **B196**, 189 (1982).
 [47] V. A. Miransky and K. Yamawaki, Phys. Rev. **D55**, 5051 (1997).
 [48] T. Appelquist, J. Terning, and L. C. R. Wijewardhana, Phys. Rev. Lett. **77**, 1214 (1996).
 [49] J. Braun and H. Gies, [JHEP 06](#), 024 (2006).

- [50] J. Braun and H. Gies, Phys. Lett. **B645**, 53 (2007).
- [51] S. Roessner, C. Ratti, and W. Weise, Phys. Rev. **D75**, 034007 (2007).
- [52] K. Fukushima and Y. Hidaka, hep-ph/0610323.
- [53] A. Dumitru and R. D. Pisarski, Phys. Rev. **D66**, 096003 (2002).
- [54] A. Dumitru, Y. Hatta, J. Lenaghan, K. Orginos, and R. D. Pisarski, Phys. Rev. **D70**, 034511 (2004).
- [55] M. LeBellac, *Thermal Field Theory* (Cambridge University Press, 1996).
- [56] C. Sasaki, B. Friman, and K. Redlich, hep-ph/0702025.
- [57] O. Kaczmarek and F. Zantow, Eur. Phys. Jour. **C43**, 63 (2005).
- [58] O. Kaczmarek and F. Zantow, Phys. Rev. **D71**, 114510 (2005).
- [59] M. Cheng, N. H. Christ, S. Datta, J. van der Heide, C. Jung, F. Karsch, O. Kaczmarek, E. Laermann, R. D. Mawhinney, C. Miao, et al., Phys. Rev. **D74**, 054507 (2006).
- [60] Y. Aoki, Z. Fodor, S. D. Katz, and K. K. Szabo, Phys. Lett. **B643**, 46 (2006).
- [61] B.-J. Schaefer and J. Wambach, Phys. Rev. **D75**, 085015 (2007).
- [62] P. de Forcrand and O. Philipsen, JHEP **0701**, 077 (2007); P. de Forcrand and O. Philipsen, Nucl. Phys. **B673**, 170 (2003); P. de Forcrand and O. Philipsen, Nucl. Phys. **B642**, 290 (2002).
- [63] A. Ali Khan et al. (CP-PACS), Phys. Rev. **D64**, 074510 (2001).
- [64] C. R. Allton, M. Doering, S. Ejiri, S. J. Hands, O. Kaczmarek, F. Karsch, E. Laermann, and K. Redlich, Phys. Rev. **D71**, 054508 (2005).
- [65] C. Ratti, S. Roessner, M. A. Thaler, and W. Weise, Eur. Phys. J. **C49**, 213 (2007).
- [66] F. Karsch and E. Laermann, Phys. Rev. **D50**, 6954 (1994).
- [67] C. R. Allton, S. Ejiri, S. J. Hands, O. Kaczmarek, F. Karsch, E. Laermann, and C. Schmidt, Phys. Rev. **D66**, 074507 (2002).